Studying Quantum Dot Blinking through the Addition of an Engineered Inorganic Hole Trap

Ron Tenne,[†,§] Ayelet Teitelboim,[†,§] Pazit Rukenstein,[‡] Maria Dyshel,[†] Taleb Mokari,[‡] and Dan Oron[†,*]

[†]Department of Physics of Complex Systems, Weizmann Institute of Science, Rehovot 76100, Israel and [‡]Department of Chemistry and Ilse Katz Institute for Nanoscience and Nanotechnology, Ben-Gurion University of the Negev, Beer Sheva, Israel. [§]Ron Tenne and Ayelet Teitelboim contributed equally. R.T., A.T., and M.D. performed the optical experiments. Nanoparticles were synthesized and characterized by P.R. The work was conceived and supervised by T.M. and D.O. The manuscript was written by R.T. and A.T. with significant contributions of all authors. All authors have given approval to the final version of the manuscript.

ABSTRACT An all-inorganic compound colloidal quantum dot incorporating a highly emissive CdSe core, which is linked by a CdS tunneling barrier to an engineered charge carrier trap composed of PbS, is designed, and its optical properties are studied in detail at the single-particle level. Study of this structure enables a deeper understanding of the link between photoinduced charging and surface trapping of charge carriers and the phenomenon of quantum dot blinking. In the presence of the hole trap, a "gray" emissive state appears, associated with charging of the core. Rapid switching is observed between the "on" and the "gray" state, although the switching dynamics in and out of the dark "off" state remain unaffected. This result completes the links in the causality chain connecting charge carrier trapping, charging of QDs, and the appearance of a "gray" emission state.

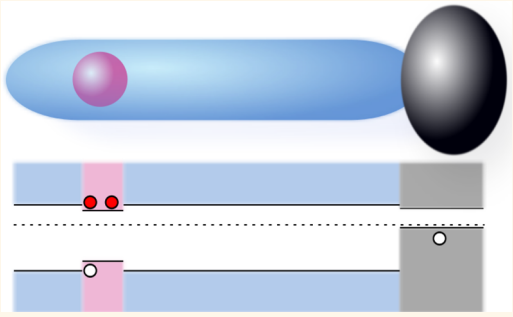

KEYWORDS: blinking · quantum dots · charge transfer · trapped states · "gray" state

Fluorescence intermittency, also termed blinking, refers to the digital-like fluctuations in the luminescence intensity of single light emitters over time. The phenomenon, first observed in atoms[1,2] and organic molecules,[3] occurs also in inorganic nanostructures such as nanowires[4] and colloidal quantum dots (QDs).[5] In QDs in particular, in which long dark periods occur often, blinking is a major drawback for applications such as particle tracking, single photon sources, and labels for biological imaging.

Since QD blinking was found to be robust to changes in the constituent materials and QD size, the notion of a universal model accounting for the dark "off" state, suggested by Efros and Rosen, was well accepted.[6] The dark state was claimed to be the result of QD charging, allowing nonradiative relaxation through a trion Auger process, whereby an exciton recombines while transferring its excess energy to the third spectator charge. Upon neutralization of the QD, radiative recombination is reconstituted and the exciton energy is released as a photon.

One of the most surprising features of QD blinking is the switching dynamics; the distribution of "off" and "on" state durations follows a power law extending over several orders of magnitude in time,[7] cut off by an exponential tail only at very long time intervals. To account for this broad distribution, with no characteristic time scale, the Auger mechanism was expanded to include charging through multiple charge traps,[8] dynamical trapping rates,[9−11] or diffusion of ejected electrons back to the QD.[12] While all models differ in the underlying mechanism for switching, they all rely on the Auger process as the darkening mechanism during the "off" state.

On the basis of the Auger mechanism, a few strategies toward nonblinking QDs were developed,[13−15] aimed at decreasing the rate of Auger recombination or restricting the charge carrier from surface states that can serve as charge traps. In thick-shelled CdSe/CdS QDs exhibiting suppressed blinking, Spinicelli *et al.*[16] found that the darkest periods exhibit a high 19% quantum yield (QY) and referred to it

* Address correspondence to dan.oron@weizmann.ac.il.

Received for review February 7, 2013 and accepted May 13, 2013.

Published online May 13, 2013
10.1021/nn4017845

as "gray" state periods. This measured QY is more than an order of magnitude higher than that of a typical dark "off" state in, for example, CdSe/CdS/ZnS QDs.[17] Thus, the question whether the Auger mechanism could indeed be responsible for such a range of values was raised.

During the past few years several works displayed experimental results challenging Auger-based blinking models.[17−20] One of these innovative measurement techniques employs electrochemistry to measure *in situ* fluorescence during QD charging.[19,21,22] By tuning the voltage of a transparent electrode onto which QDs are adsorbed, the QDs can be loaded with an extra electron. One of the main findings of these studies is that the QY of a negatively charged QD is often not sufficiently low to account for the drastically reduced emission measured in the "off" state. Qin *et al.*[20] combined that realization with the aforementioned observation of a "gray" state in CdSe/CdS QDs and arrived at the conclusion that the "gray" state, and not the "off" state, is the result of negative charging of a QD. It was furthermore shown in that work that a "gray" state is a short-lived one with a duration distribution cutoff at ~10 ms, unlike the broad power-law distribution of the "off" state duration.

Although charging was neatly tied with the occurrence of a "gray" state, the route by which QDs become charged through trapping was not elucidated. A possible pathway to clarify the role of trapping is to controllably add trap states to the QD surface and observe QY quenching. The use of chemically linked organic dye molecules to induce charge transfer in general[23] and electron transfer in particular[24] was indeed shown to diminish fluorescence. However, using organic ligands, adequate control over the number of traps attached to a QD is difficult to achieve.

We propose here a different approach to induce charging; a fully inorganic NR heterostructure that is essentially composed of two isolated QDs separated by a tunneling barrier, where one serves as an optical emitter while the other serves as a controlled charge carrier trap. The particular system realized here is based on a CdSe/CdS seeded rod onto which a PbS tip was grown. The tip component serves as a localized hole trap, facilitating the effective charging of the optically active QD core. Such architecture allows for examination of QD blinking under stochastic charging conditions resulting from the designed trap state.

RESULTS AND DISCUSSION

A schematic drawing of the system presented in this work, complying with the requirements mentioned above, is shown in Figure 1a with its energy band diagram given below. A 9 × 12 nm PbS nanocrystal (NC) was selectively grown on the tip of a CdSe/CdS seeded NR with a 3.7 nm core and a total length of about 70 nm and 4 nm width. A detailed description of the growth procedure appears in the Methods section and in ref 25.

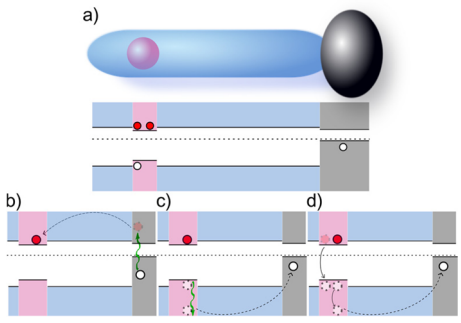

Figure 1. (a) A schematic of a PbS-tipped CdSe/CdS seeded rod, alongside its corresponding energy band diagram. The formation of electrons (red) and holes (white) depicts their locations during a charged state; a hole is trapped within the PbS tip, while an extra electron inhabits the core. (b−d) Three proposed mechanism by which an electron can be injected into the CdSe core, while a hole is left trapped in the PbS tip. (b) Injection of a hot electron, from an exciton originated in the PbS tip, into the core. (c, d) Migration of a hot hole from the core to the PbS tip. (c) Heating of a cold hole *via* intraband absorption. (d) Generation of a hot hole by Auger recombination in the core.

Due to the band alignment of the three components, the valence band potential landscape is of a double-well formation, in which the long CdS rod serves both as an energetic barrier inhibiting tunneling and as a physical barrier practically eliminating intraparticle FRET. PbS is a narrow band gap semiconductor. This property combined with the characteristics of the CdS/PbS heterostructure, in which the Fermi energy of CdS is shifted toward the conduction band, as opposed to that of PbS, which is shifted toward the valence band, results in a band alignment that produces an energetically deep hole trap with delocalization of electrons in the conduction band;[26,27] see Supporting Information for XPS results of the NC valence band alignments.

A numerical solution of the Schrödinger equation under the effective mass approximation, taking into account a 300 meV offset in the bulk values of the conduction band of a CdSe/CdS interface,[28] shows that the excited electron's lowest energy level is about ~80 meV below the bulk conduction level energy in CdS. As a result, the electron's wave function in this state decays exponentially into the CdS barrier with a characteristic length scale of ~2 nm. This means that while the electron is not restricted to the CdSe core, in our system, in which the rod's length is ~70 nm, the electron certainly does not tunnel to the tip of the NC even considering thermal excitations.[29−31]

The mechanism by which an electron can be injected into the CdSe core while a hole is left trapped in the PbS tip can be suggested by the CdSe/CdS PbS-tipped hetrostructure band alignment. This indicates that the charging mechanism can occur in one of three ways. A hot electron can be injected from an exciton

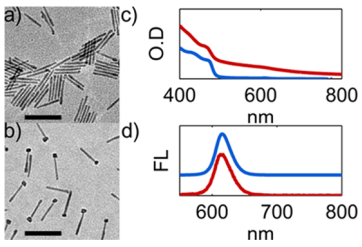

Figure 2. (a, b) TEM images of CdSe/CdS-seeded rods (a) and PbS-tipped CdSe/CdS-seeded rods (b). The scale bar is 100 nm. (c) Absorption spectra of the bare NRs (blue) and PbS-tipped NRs (red). (d) Fluorescence spectra following the same color code as in (c). Curves were vertically shifted for clarity.

formed in the PbS tip to the core. This is facilitated by the relatively flat conduction band alignment between the PbS tip and the CdS rod and the fact that we excite the PbS with a high-energy photon relative to its band gap. This is a relatively robust effect that has been shown to depend little on the PbS tip size[34] and is not expected to strongly depend on the length of the NR. Alternatively, a hot hole can go in the opposite direction from the core to the PbS tip. The hundreds of meV scale barrier together with the large physical distance render the latter transition practically impossible after the core exciton has cooled. The two possible sources of hot holes are thus heating of cooled charge carriers *via* photoactivated intraband transitions[35] or the generation of hot carriers by Auger recombination in the core.[36] The three possible charging mechanisms are illustrated in Figure 1b–d. It can be concluded that the most probable charging mechanism is the injection of a hot electron from an exciton originated in the PbS tip.

Figure 2a and b present transmission electron microscopy (TEM) images of CdSe/CdS-seeded rods and PbS-tipped CdSe/CdS NRs, referred to throughout this work as bare NRs and PbS-tipped NRs, respectively. The nanocrystals display a high degree of homogeneity in size and shape of the NRs as well as selective growth of PbS on the NR tip alone. Figure 2c and d depict the absorption and normalized fluorescence spectra of the bare and the PbS-tipped NRs in blue and in red, respectively. While the absorption curve develops a red tail with the addition of PbS tips, the fluorescence line shape and peak position in the visible spectrum remain unchanged. This indicates that, as mentioned above, visible photons originate from exciton recombination in the CdSe core, and therefore the energetics of emission is unchanged by the tip growth. It should be noted that for this size, PbS emission is expected to be deep into the near-infrared range of the spectrum, around 1.8 μm.[37]

The experimental setup for single QD spectroscopy is described in the Methods section in full detail. Briefly, the fluorescence signal from single NCs was measured in an epi-fluorescence setup using 100 fs, 528 nm excitation pulses at 80 MHz, obtained from a doubled Ti:Sapphire oscillator. Fluorescence of single

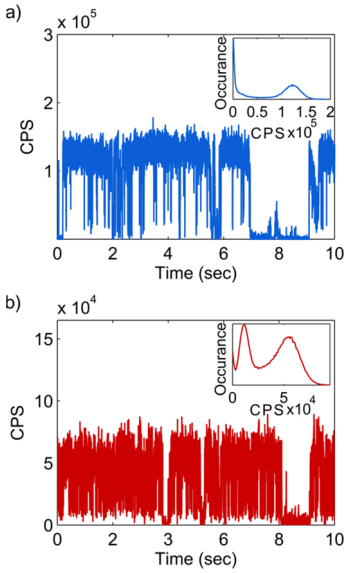

Figure 3. Fluorescence signal time trace of a single bare NR (a) and a PbS-tipped one (b) during a 10 s period, binned at a 1 ms resolution. Insets present an intensity histogram, the occurrence of fluorescence intensities, compiled from the full blinking trace. While both histograms have one peak at a close to zero count rate and a second one at high intensities, the PbS-tipped QD displays a third peak at an intermediate intensity.

QDs embedded within a PMMA film was collected through an objective lens, spectrally separated from the excitation beam and measured using two avalanche photodiodes in a Hanbury-Brown and Twiss setup. The signal from the two detectors was collected by a dual-channel time-correlated single photon counting module. A measured trace was deemed to be from a single NC based on the antibunching feature in its second-order autocorrelation function (see Supporting Information). Data obtained from emitters for which the antibunching dip did not go below 40% were discarded, as those are likely not single nanoparticles.

Figure 3 visualizes the qualitative essence of this work, featuring fluorescence signal curves over time for a single representative bare NR (a) and a PbS-tipped one (b) at a 1 ms temporal resolution. From this comparison one can observe that while in both cases switching occurs between three intensity states, the intermediate state occurs substantially more frequently in the PbS-tipped case. To receive a clearer impression of this change, the insets of Figure 3 provide the occurrence (*i.e.*, time spent) *vs* intensity curves. Indeed, three peaks, representing the three states, are present only for the PbS-tipped NR. The intermediate, "gray", state peak is located at ~20% of the brightness of the "on" state, while the "off" state peak is at about 1%, corresponding to 1000 counts per second, on the order of the detector's dark current count rate.

Other than recognizing the three different states, Figure 3 also demonstrates the drastically modified dynamics of switching between the three states.

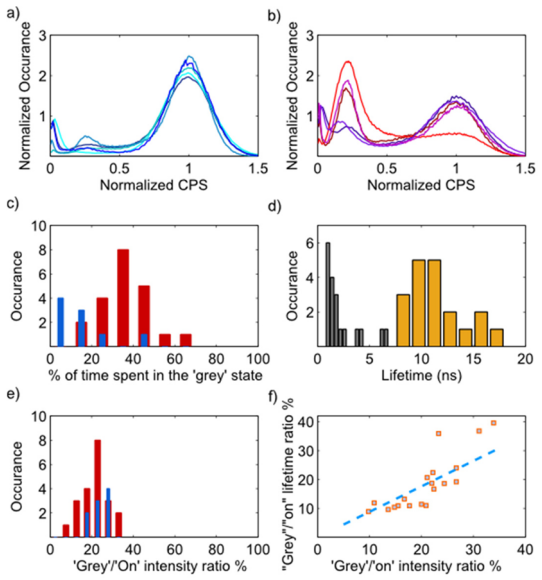

Figure 4. Ensemble statistics for bare NRs and PbS-tipped NRs. (a, b) Intensity histograms of five different bare NRs (left) and PbS-tipped ones (right). (c) Distribution of the portion of time spent in a "gray" state for bare (blue) and PbS-tipped (red) NRs. (d) Distribution of decay lifetime for the "on" (orange) and "gray" (gray) states of PbS-tipped NRs constructed by single-exponential fitting of the corresponding state's decay curve. (e) Ratio of "gray" to "on" peak count rate for bare (blue) and PbS-tipped (red) NRs. (f) Scatter plot of the "gray" to "on" lifetime ratio *vs* the "gray" to "on" fluorescence intensity ratio for PbS-tipped NRs. A linear fit (blue dashed line) highlights the positive, approximately linear, correspondence between the two ratios.

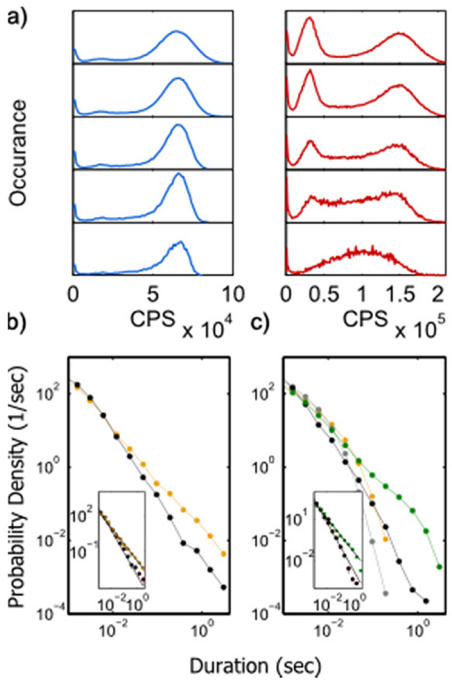

Figure 5. (a) Intensity histograms of the same trace composed with increasing binning width from top to bottom panel of 1, 2, 5, 10, and 30 ms. The left row (blue) is for a single bare NR, whereas the right row (red) is for a PbS-tipped NR. Duration histograms of the different states for a single bare NR and a single PbS-tipped NR are given in (b) and (c), respectively, on a log−log scale. Both panels contain the "on" (orange) and "off" (black) state curves, whereas the "gray" state distribution (gray) is shown only for the PbS-tipped NR. Additionally, we plot for the PbS-tipped NRs the probability distribution for non-"off" (*i.e.*, both "gray" and "on") states joined together (green). Insets of both panels present power law fits of the "on" (power −1.2) and "off" (power −1.8) distribution in (b) and for the joined "on" and "gray" state (power −1.3) and the "off" state (power −1.9) distributions in (c).

In particular, switching times between "gray" and "on" state are very rapid, on a millisecond time scale, in stark contrast with "off" state durations, which are known for not having any characteristic time scale.

At this point we mention that ~80% of the measured PbS-tipped NRs exhibit the behavior presented in Figure 3. For the analyses given below, we chose to work only with NRs for which the three peaks in the intensity histogram were clearly separated.

Quantitative corroboration of the two features described above is shown in Figures 4 and 5. First, the addition of PbS enhances the occurrence of an existing "gray" state in CdSe/CdS rods without affecting the occasional switching into the "off" state. Second, the "gray" state is a short-lived one with a typical time scale of 10 ms, unlike the "off" state, whose duration distribution follows a power law.

The first of these two points is clearly seen in Figures 4a and 4b, which compare the typical normalized intensity distribution functions for single bare NRs (a) with those of single PbS-tipped ones (b). To provide a graphic visualization of the variance between particles, five curves of each are shown (while a statistical characterization of the measured ensemble appears hereafter). The *x* values of the curves were normalized so that the "on" state peak center occurs at unity in order to compensate for the distribution of absorption cross sections. One can notice that while some of the bare NRs' curves exhibit a small "gray" state peak, the PbS-tipped NRs spend an appreciable amount of time in the "gray" state. This observation is quantified in Figure 4c, which presents the distribution of the percentage of time NCs spent in the "gray" state. The blue bars represent the bare NRs ensemble, which are mostly below 20%, while the PbS-tipped NRs, shown in red, are centered around 40%.

A diminished brightness state can be the consequence of a decreased absorption rate, hot carrier trapping, or nonradiative recombination of band-edge excitons. The last option manifests itself in a drop of the observed emission lifetime resulting from the opening of a high-rate nonradiative recombination channel. Figures 4d−f reveal that, indeed, the "gray" state's diminished brightness stems from an extra nonradiative recombination mechanism for the band-edge excitons.

Figure 4d presents the distribution of exciton lifetime in the "gray" and "on" state, extracted by exponential fitting of the decay curve of the corresponding

state. A decay curve for a specific state was composed from detection events postselected according to a brightness range centered at the state's peak in the intensity histogram. While the distribution of decay times during the "on" state is centered at 10 ns, the matching distribution during the "gray" state is focused around 2 ns, approximately 20% of the radiative lifetime. The distribution of "gray" to "on" state fluorescence intensity ratio is given in Figure 4e, showing that in this case, as well, values cluster around 20%. The correlation between the lifetime ratio and the brightness ratio of the "gray" to "on" state is shown in Figure 4f, displaying a linear correlation between the decline in lifetime during the "gray" state and the reduction of the fluorescence signal.

This correlation asserts the claim that the dimness of the "gray" state is the result of an additional recombination mechanism operating only when the NR is in the "gray" state. The association of the "gray" state specifically with the negative trion Auger process is supported by the estimate of biexciton Auger lifetime deduced from transient absorption measurements and the antibunching analysis (see Supporting Information). The biexciton Auger lifetime was found to be ~0.5 ns by the transient absorption measurements, approximately 25% of the "gray" state emission lifetime. Since the holes are more highly localized in the CdSe/CdS system, negative trion Auger lifetimes have been shown to be a factor of 6−7 larger than those of the biexciton,[32] in reasonable agreement with our observations.

In order to support the second point mentioned above, further analyses were aimed to address the switching dynamics from one state to another. Figure 5a depicts intensity histograms of the same NC blinking trace with varying binning resolution. By increasing the bin width in the compilation of the blinking trace, short events can be missed and some bins may contain a mixture of a few states together. While for the bare NR traces depicted in the left column no appreciable change occurs with varying bin width, for the PbS-tipped NRs it is noticeable that at a bin width of 30 ms the two peaks, for the "on" and "gray" state, merge together to create one broad peak. The generated broad peak is caused by a majority of 30 ms bins containing both "on" and "gray" periods, which implies that durations of the "on" and "gray" state events for these NCs are relatively short.

For a more accurate characterization of the switching time scale between different states, the duration distributions for the states present in a single bare NR and a single PbS-tipped NR are presented in Figure 5b and c, respectively, on a log−log scale. The "off" state distributions (black) follow a distinct power law matching the commonly reported distribution[7,33] for both the bare NR and the PbS-tipped one. However, for the "on" state (orange) a distinct cutoff at a scale of 10 ms is introduced with the addition of the PbS tip. This short

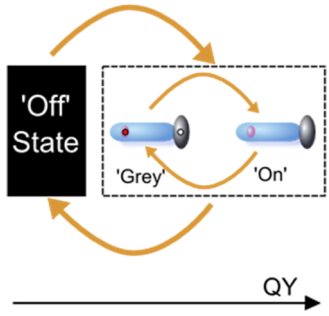

Figure 6. Switching dynamics between the three states: "on", "gray", and "off". Two independent transitions occur in the QD, the first into and out of the dark "off" state and the second between the "on" state and the single electron charged "gray" state.

time cutoff is present in the "gray" state as well (gray). In order to show that the "gray" state emerges at the expense of the "on" state alone, we plot the duration distribution for the "on" and "gray" states joined together (green). While each of the components states ("gray" and "on") exhibit a cutoff, the joint distribution follows a power law with approximately the same power as for the "on" state in the bare NR. We have ensured that this result is independent of the particular choice of threshold values. This observation indicates that there are two independent switching processes occurring in this system. The QD switches into and out of the dark state with a power law statistics, and while it is in the bright state it experiences a second kind of blinking from the "on" to the "gray" state.

In their work Qin *et al.*[20] used the different dynamics of the "gray" and "off" state to resolve the two and estimate an exponential cutoff for the "gray" state at 6 ms. The qualitative agreement in the "gray" state duration cutoff between Qin's work and our work hints that a long-lived trapped state might be hard to achieve. Even an energetically deep and physically long trap does not last for more than 30 ms in our NRs, 3 orders of magnitude below the tens of seconds' duration regularly measured for long "off" intervals.

CONCLUSIONS

Figure 6 contains a summary of our findings presented from a mechanistic point of view. We show here, for the first time, a QD fluctuating between three distinct brightness states. The intermediate brightness, "gray" state appears after the addition of a PbS tip to the CdSe/CdS NR.

We presented a few indications that the "gray" state is the result of stochastic negative charging of the QD, through the trapping of a hole in the PbS tip. First, the 20% brightness of this state compared with that of the "on" state matches values reported in the literature for the lifetime reduction of a charged thick-shelled CdSe/CdS QD.[20] Second, reduced brightness events are accompanied with proportional emission lifetime decrease, proving that this reduction is the result of a

nonradiative recombination route present only during the "gray" state. Finally, we found that this lifetime matches an approximation of the negative trion Auger lifetime occurring in a single electron charged QD as proposed by the trapping mechanism.

The "gray" state profoundly differs from the "off" state in its switching dynamics. As portrayed in Figure 6, two transitions, manifested in the QD's fluorescence signal, occur independently: one, into and out of the dark "off" state and the other between the "on" state and the charged "gray" state. While the first transition is a subject of extensive debate in the literature, we can state here that charging, through carrier trapping, is not the reason for darkening during the "off" state in this system since the induction of charging through the addition of a designed hole trap did not change the relative occurrence of the "off" state.

The connection between charging, fluorescence quenching, and emission lifetime reduction in QDs has been previously shown.[19,20] Also, the appearance of a "gray" state has been measured in CdSe/CdS NCs and explained by a negatively charged state occurring through charge carrier trapping.[16,20] Here we manage to link the full causality chain between charge carrier trapping, negative charging of the QD, and the occurrence of a "gray" state.

In summary, we have shown a clear transition in the type of blinking that occurs in a CdSe/CdS NR with the addition of a PbS tip in two aspects: the enhanced occurrence of a "gray" state and the dramatically faster switching dynamics between the "gray" and "on" states. We therefore propose that this transition results from the stochastic trapping of holes within the PbS tip, which causes an effective charging of the QD, leading to a diminished fluorescence, "gray" state. While this work focused on the consequences of this transition regarding the blinking mechanism, such a transition can perhaps be tailored to suit a specific application using different QD geometries and choice of constituent materials. Specifically, super-resolution imaging based on fluorescence fluctuations[38] stands to benefit from frequent fluctuations between two, above noise, luminescence states ("gray" and "on"), and particle tracking applications could improve if fluorescence fluctuations occur mainly on a short time scale below the exposure time of a frame.

METHODS

Synthesis. CdSe seeds synthesis: 3.0 g of TOPO, 0.280 g of ODPA, and 0.060 g of CdO were mixed in a 50 mL flask and heated to 150 °C under a nitrogen atmosphere for an hour. After heating to 300 °C, 1.5 g of TOP was injected into the solution. Following a temperature raise to 380 °C, 0.058 g of Se, dissolved in 0.360 g of TOP, was injected. Immediately after the injection, the heating mantle was removed and the solution was cooled to room temperature.

The CdSe/CdS rods were synthesized according to a previously published report. For detailed information, see the Supporting Information. The dimensions of the CdSe/CdS-seeded rods main axes were estimated as 70 × 4 × 4 nm.

Selective growth of PbS tips on CdSe/CdS NRs: CdSe/CdS NRs (OD 1 at the first excitonic transition, 462 nm) were mixed with 3 mg of Pb-bisdiethyldithiocarbamate and 3 mL of TOP. The mixture was heated to 213 °C for 3 min. The reaction was then stopped by removing the heating mantle and allowing the solution to be cooled to room temperature.

A more detailed description of the synthesis is given in ref 25 and in the Supporting Information.

Sample Preparation. A dilute solution of NCs in toluene was ultrasonicated for 10 min and mixed into a 2% w/v solution of PMMA in toluene. The solution was immediately spin coated onto a glass coverslip, forming a QD embedded thin film of PMMA, in which NCs are typically spatially separated by more than 5 μm.

Optical Imaging System. As an excitation source a Ti:Sapphire laser (Coherent Chameleon), emitting 100 fs pulses at 1056 nm wavelength at an 80 MHz repetition rate, was used. The beam was frequency doubled using a BBO crystal (MT Berlin) to create a 528 nm beam, from which the fundamental was eliminated by a combination of a bandpass filter 534/30 (Semrock) and a Schott heat-absorbing color glass filter. The beam was expanded using a Galilean Zoom beam expander (BE02-05A Thorlabs).

Single-dot optical measurements were performed using a custom-built optical characterization system based on a commercial inverted microscope (Zeiss Axiovert 200). Imaging of the whole field of view was achieved by using a wide field illumination of a 455 nm blue diode (Mightex). Photoluminescence was imaged through an oil-immersed objective (Zeiss Plan Apochromat X63 NA 1.4) onto an electron-multiplying CCD camera (Acton-PI PhotonMax 512). Excitation of a single QD was done using a tightly focused beam of 528 nm. The excitation beam was reflected from a dichroic mirror (Omega optical 567LP) into an oil immersion objective that focused the light into a diffraction-limited spot in the sample plane. The polarization of the laser beam was tuned to circular using a liquid crystal phase retarder (LCR-1-NIR Thorlabs), to ensure uniform excitation of the NRs regardless of their spatial orientation.

Fluorescent photons (centered on 610 nm) were collected through the same objective, spectrally filtered by a bandpass filter 609/57 (Semrock), and imaged onto the entrance of a multimode fiber splitter (F-CPL-M12855 Newport) dividing the signal into two single-photon avalanche photodiodes (Perkin-Elmer SPCM). The two detectors together with the trigger output of the laser were connected to a multiple-channel time-correlated single-photon counting system (Picoquant HydraHarp 400), enabling both coincidence analysis and lifetime measurements.

Measurements were postselected according to their second-order autocorrelation curves ($g^{(2)}$). Only QDs for which the $g^{(2)}$ dip at zero time delay was lower than 40% were processed as single QDs, thus assuring that only fully single NC traces would be taken into account (see the Supporting Information for more details).

Conflict of Interest: The authors declare no competing financial interest.

Acknowledgment. The authors would like to acknowledge support from the ERC starting grants SINSLIM (258221, DO group) and Nano@Energy (278779, TM group). Financial support by the Minerva Foundation is gratefully acknowledged. D.O. is the incumbent of the Recanati career development chair in energy research. The authors would like to thank Iddo Pinkas for his help with transient absorption measurements and Hagai Cohen for his help with XPS measurements.

Supporting Information Available: This material is available free of charge *via* the Internet at http://pubs.acs.org.

REFERENCES AND NOTES

1. Nagourney, W.; Sandberg, J.; Dehmelt, H. Shelved Optical Electron Amplifier: Observation of Quantum Jumps. *Phys. Rev. Lett.* **1986**, *56*, 2797–2799.
2. Bergquist, J.; Hulet, R.; Itano, W.; Wineland, D. Observation of Quantum Jumps in a Single Atom. *Phys. Rev. Lett.* **1986**, *57*, 2–5.
3. Basché, T.; Kummer, S.; Bräuchle, C. Direct Spectroscopic Observation of Quantum Jumps of a Single Molecule. *Nature* **1995**, *373*, 132–134.
4. Protasenko, V.; Gordeyev, S.; Kuno, M. Spatial and Intensity Modulation of Nanowire Emission Induced by Mobile Charges. *J. Am. Chem. Soc.* **2007**, *129*, 13160–13171.
5. Nirmal, M.; Dabbousi, B.; Bawendi, M. Fluorescence Intermittency in Single Cadmium Selenide Nanocrystals. *Nature* **1996**, *383*, 802–804.
6. Efros, A.; Rosen, M. Random Telegraph Signal in the Photoluminescence Intensity of a Single Quantum Dot. *Phys. Rev. Lett.* **1997**, *78*, 1110–1113.
7. Frantsuzov, P.; Kuno, M.; Janko, B.; Marcus, R. A. Universal Emission Intermittency in Quantum Dots, Nanorods and Nanowires. *Nat. Phys.* **2008**, *4*, 519–522.
8. Verberk, R.; van Oijen, A.; Orrit, M. Simple Model for the Power-Law Blinking of Single Semiconductor Nanocrystals. *Phys. Rev. B* **2002**, *66*, 233202.
9. Shimizu, K.; Neuhauser, R.; Leatherdale, C.; Empedocles, S.; Woo, W.; Bawendi, M. Blinking Statistics in Single Semiconductor Nanocrystal Quantum Dots. *Phys. Rev. B* **2001**, *63*, 1–5.
10. Tang, J.; Marcus, R. Diffusion-Controlled Electron Transfer Processes and Power-Law Statistics of Fluorescence Intermittency of Nanoparticles. *Phys. Rev. Lett.* **2005**, *95*, 107401.
11. Kuno, M.; Fromm, D. P.; Hamann, H. F.; Gallagher, A.; Nesbitt, D. J. "On"/"off" Fluorescence Intermittency of Single Semiconductor Quantum Dots. *J. Chem. Phys.* **2001**, *115*, 1028–1040.
12. Margolin, G.; Protasenko, V.; Kuno, M.; Barkai, E. L. Power-law blinking quantum dots: stochastic and physical models. In *Fractals, Diffusion, and Relaxation in Disordered Complex Systems: Advances in Chemical Physics*, Part A; Wiley-Interscience, 2006; Vol. 133, pp 327–356.
13. Mahler, B.; Spinicelli, P.; Buil, S.; Quelin, X.; Hermier, J.-P.; Dubertret, B. Towards Non-blinking Colloidal Quantum Dots. *Nat. Mater.* **2008**, *7*, 659–664.
14. Wang, X.; Ren, X.; Kahen, K.; Hahn, M. A.; Rajeswaran, M.; Maccagnano-Zacher, S.; Silcox, J.; Cragg, G. E.; Efros, A. L.; Krauss, T. D. Non-blinking Semiconductor Nanocrystals. *Nature* **2009**, *459*, 686–689.
15. Chen, Y.; Vela, J.; Htoon, H.; Casson, J. L.; Werder, D. J.; Bussian, D. A.; Klimov, V. I.; Hollingsworth, J. A "Giant" Multishell CdSe Nanocrystal Quantum Dots with Suppressed Blinking. *J. Am. Chem. Soc.* **2008**, *130*, 5026–5027.
16. Spinicelli, P.; Buil, S.; Quélin, X.; Mahler, B.; Dubertret, B.; Hermier, J.-P. Bright and Grey States in CdSe-CdS Nanocrystals Exhibiting Strongly Reduced Blinking. *Phys. Rev. Lett.* **2009**, *102*, 136801.
17. Rosen, S.; Schwartz, O.; Oron, D. Transient Fluorescence of the Off State in Blinking CdSe/CdS/ZnS Semiconductor Nanocrystals Is Not Governed by Auger Recombination. *Phys. Rev. Lett.* **2010**, *104*, 157404.
18. Zhao, J.; Nair, G.; Fisher, B. R.; Bawendi, M. G. Challenge to the Charging Model of Semiconductor-Nanocrystal Fluorescence Intermittency from Off-State Quantum Yields and Multiexciton Blinking. *Phys. Rev. Lett.* **2010**, *104*, 157403.
19. Galland, C.; Ghosh, Y.; Steinbrück, A.; Sykora, M.; Hollingsworth, J. A.; Klimov, V. I.; Htoon, H. Two Types of Luminescence Blinking Revealed by Spectroelectrochemistry of Single Quantum Dots. *Nature* **2011**, *479*, 203–207.
20. Qin, W.; Guyot-Sionnest, P. Evidence for the Role of Holes in Blinking: Negative and Oxidized CdSe/CdS Dots. *ACS Nano* **2012**, *6*, 9125–9132.
21. Jha, P. P.; Guyot-Sionnest, P. Photoluminescence Switching of Charged Quantum Dot Films. *J. Phys. Chem. C* **2007**, *111*, 15440–15445.
22. Jha, P. P.; Guyot-Sionnest, P. Electrochemical Switching of the Photoluminescence of Single Quantum Dots. *J. Phys. Chem. C* **2010**, *114*, 21138–21141.
23. Xu, Z.; Cotlet, M. Photoluminenscence Blinking Dynamics of Colloidal Quantum Dots in the Presence of Controlled External Electron Traps. *Small* **2011**, 253–258.
24. Bang, J.; Park, J.; Velu, R.; Yoon, E.; Lee, K.; Cho, S.; Cha, S.; Chae, G.; Joo, T.; Kim, S. Photoswitchable Quantum Dots by Controlling the Photoinduced Electron Transfers. *Chem. Commun.* **2012**, *48*, 9174–9176.
25. Rukenstein, P.; Jen-La Plante, I.; Diab, M.; Chockler, E.; Flomin, K.; Moshofsky, B.; Mokari, T. Selective Growth of Metal Sulfide Tips onto Cadmium Chalcogenide Nanostructures. *Cryst. Eng. Commun.* **2012**, *14*, 7590–7593.
26. Musikhin, S.; Bakueva, L.; Sharonova, L. V. Optical Properties of PbS/CdS Superlattices Grown by Pulsed Laser Evaporation. *Superlattices Microstruct.* **1994**, *15*, 495–498.
27. Watanabe, S.; Mita, Y. Electrical Properties of CdS-PbS Heterojunctions. *Solid-State Electron.* **1972**, *15*, 5–10.
28. Sitt, A.; Della Sala, F.; Menagen, G.; Banin, U. Multiexciton Engineering in Seeded Core/Shell Nanorods: Transfer from Type-I to Quasi-Type-II Regimes. *Nano Lett.* **2009**, *9*, 3470–3476.
29. Rain, G.; Stoferle, T.; Moreels, I.; Gomes, R.; Kamal, J. S.; Hens, Z.; Mahrt, R. F. Probing the Wave Function Delocalization in CdSe/CdS Dot-in-Rod Nanocrystals by Time- and Temperature-Resolved Spectroscopy. *ACS Nano* **2011**, *5*, 4031–4036.
30. Smith, E. R.; Luther, J. M.; Johnson, J. C. Ultrafast Electronic Delocalization in CdSe/CdS Quantum Rod Heterostructures. *Nano Lett.* **2011**, *11*, 4923–4931.
31. Pisanello, F.; Leménager, G.; Martiradonna, L.; Carbone, L.; Vezzoli, S.; Desfonds, P.; Cozzoli, P. D.; Hermier, J. P.; Giacobino, E.; Cingolani, R.; *et al.* Non-Blinking Single-Photon Generation with Anisotropic Colloidal Nanocrystals: Towards Room Temperature, Efficient, Colloidal Quantum Sources. *Adv. Mater.* **2013**, *25*, 1974–1980.
32. Jha, P. P.; Guyot-Sionnest, P. Trion Decay in Colloidal Quantum Dots. *ACS Nano* **2009**, *3*, 1011–1015.
33. Schwartz, O.; Oron, D. A Present Understanding of Colloidal Quantum Dot Blinking. *Isr. J. Chem.* **2012**, *52*, 992–1001.
34. Jadhav, P. J.; Brown, P. R.; Thompson, N.; Wunsch, B.; Mohanty, A.; Yost, S. R.; Hontz, E.; Van Voorhis, T.; Bawendi, M. G.; Bulovic, M.; *et al.* Triplet Exciton Dissociation in Singlet Exciton Fission Photovoltaics. *Adv. Mater.* **2012**, *24*, 6169–6174.
35. Deutsch, Z.; Neeman, L.; Oron, D. Luminescence Upconversion in Colloidal Double Quantum Dots, submitted.
36. Seidel, W.; Titkov, A.; André, J.; Voisin, P.; Voos, M. High-Efficiency Energy Up-Conversion by an "Auger Fountain" at an InP-AlInas Type-II Heterojunction. *Phys. Rev. Lett.* **1994**, *73*, 2356–2359.
37. Moreels, I.; Lambert, I.; Smeets, D.; De Muynck, D.; Nollet, T.; Martins, J. C.; Vanhaecke, F.; Vantomme, A.; Delerue, C.; Allan, G.; *et al.* Size-Dependent Optical Properties of Colloidal PbS Quantum Dots. *ACS Nano* **2009**, *3*, 3023–3030.
38. Dertinger, T.; Colyer, R.; Iyer, G.; Weiss, S.; Enderlein, J. Fast, Background-free, 3D Super-resolution Optical Fluctuation Imaging (SOFI). *Proc. Natl. Acad. Sci. U.S.A.* **2009**, *106*, 22287–22292.